Supplement material

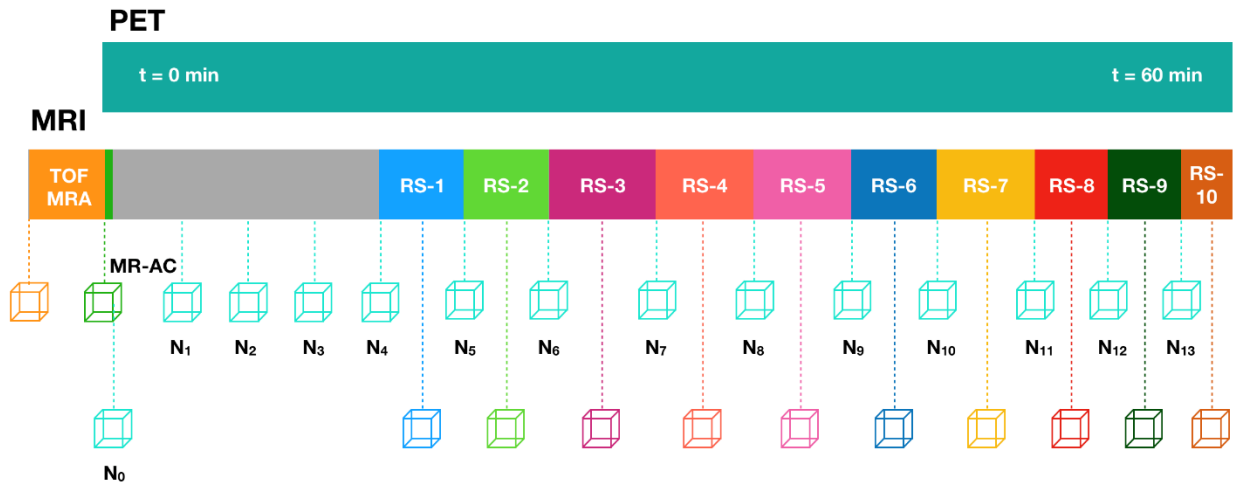

Suppl. Fig. 1 Clinical combined PET/MRI protocol: A Time-of-flight angiography (TOF-MRA) sequence was acquired prior to the start of PET acquisition followed by the acquisition of Dixon MR-attenuation map (MR-AC). A 60-min list-mode PET acquisition was initiated, with the simultaneous application of the reference MR navigator (N_0). 14 MR navigators (cyan) were interleaved between the clinical research sequences (RS-n) throughout the dynamic study to monitor subject motion.

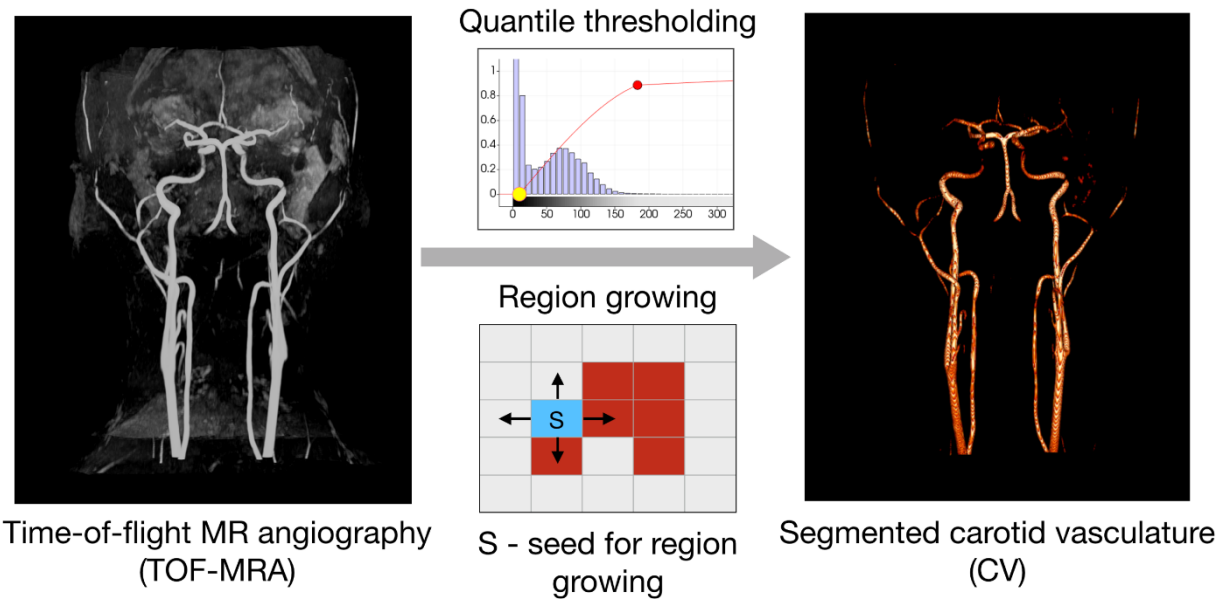

Suppl. Fig. 2. A combination of quantile based histogram thresholding (top-center) and automatic seeded region growing algorithm (top-bottom) is applied on the TOF-MRA dataset (left) resulting in a binary segmented carotid vasculature, CV (right).

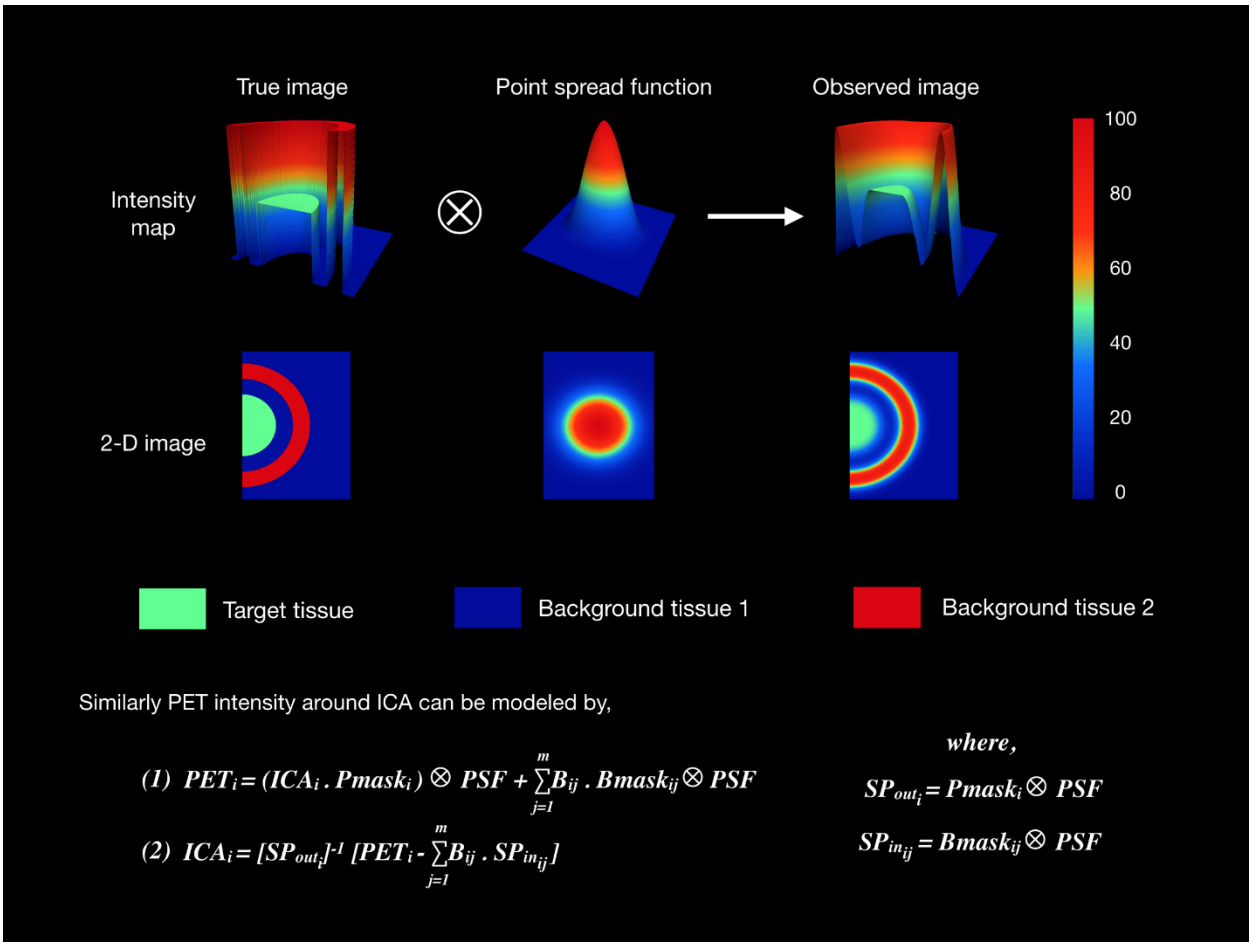

Suppl. Fig. 3. To emphasize the influence of PSF, synthetic 2-D images (bottom row) along with their intensity height map (top row) are shown. The observed PET image (right) can be considered as a convolution (⊗) of the true image (left) with the PET system's point spread function (PSF, center). The observed PET activity around the ICA can be modelled

by equation (1). To obtain the true ICA activity using equation (2), SP_{out} and SP_{in} factors were calculated by using the petrous mask ($Pmask_i$), background masks ($Bmask_{ij}$) and PET system's PSF.

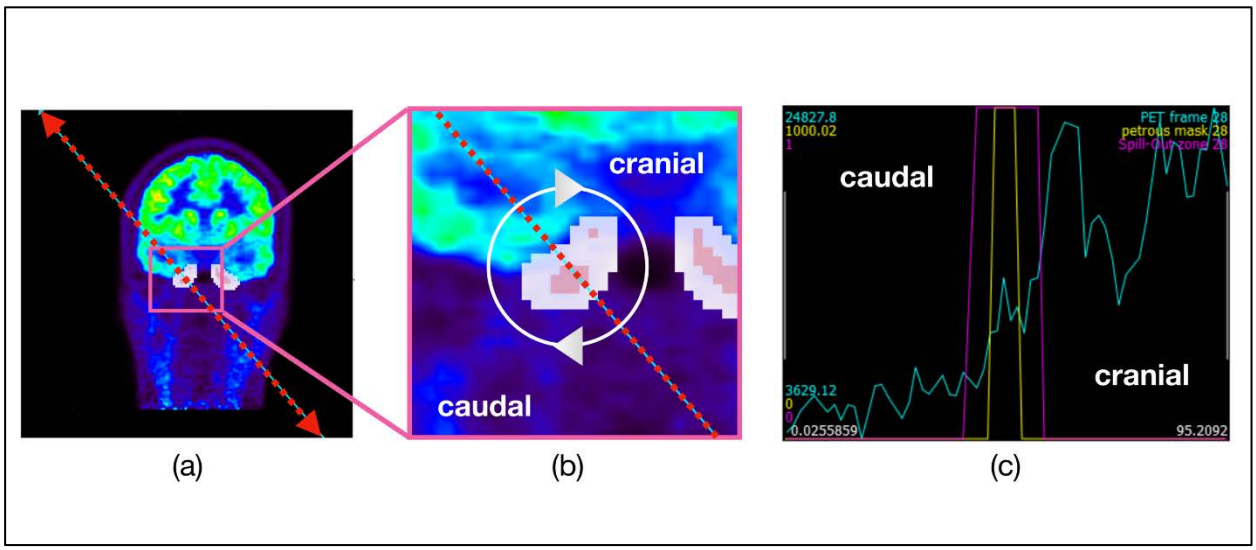

Suppl. Fig. 4. Circumferential and radial heterogeneity in a real case scenario: (a) PET frame fused with petrous (light red) and spill-out zone (white), along with the red dotted line where the activity profile was measured (b) zoom-in demonstrating the circumferential heterogeneity (white circle with arrows), as the petrous is encapsulated by the temporal lobe of the brain and the base of the skull, (c) radial activity line profile (PET – blue, petrous mask – yellow, Spill-out zone/mixed zone – magenta) illustrating the difference between the activity in the spill out zone and the immediate background.

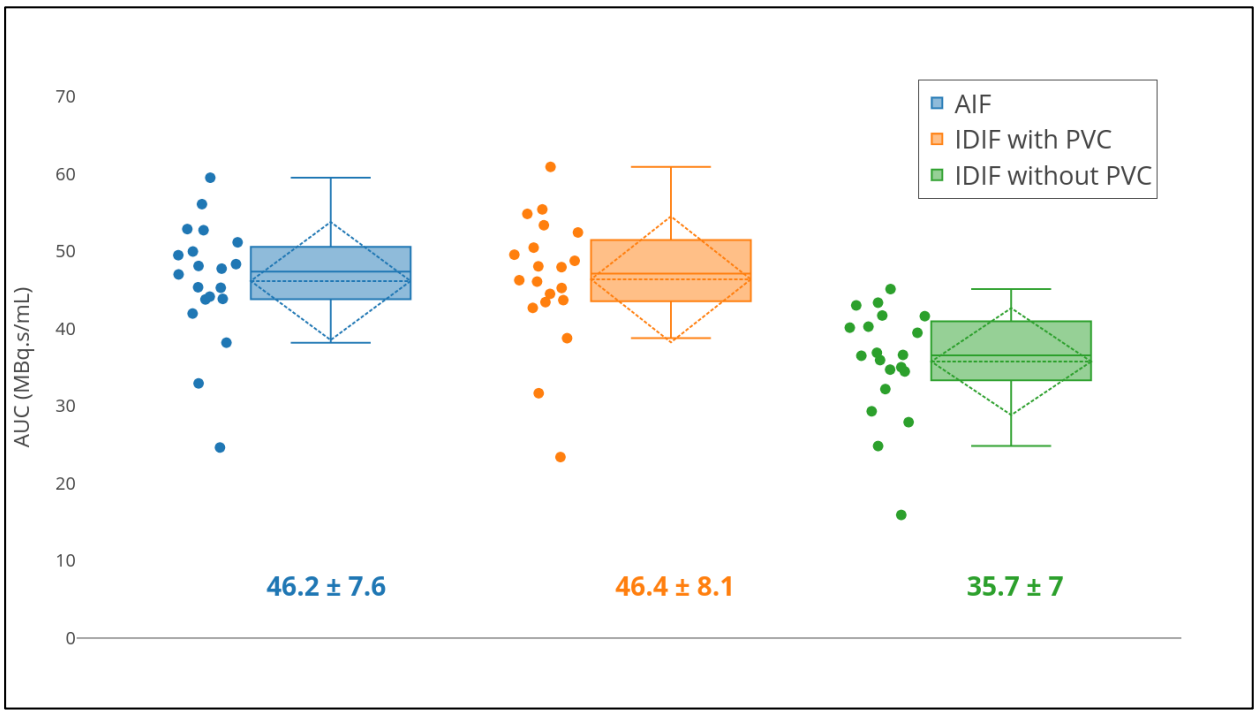

Suppl. Fig. 5. Box plots of the range of the AUCs (MBq.s/mL) of AIF (blue), IDIF after PVC (orange) and IDIF before PVC (green) along with the mean and standard deviation values. The dots adjacent to the box plot correspond to the AUC of each individual IF curve.

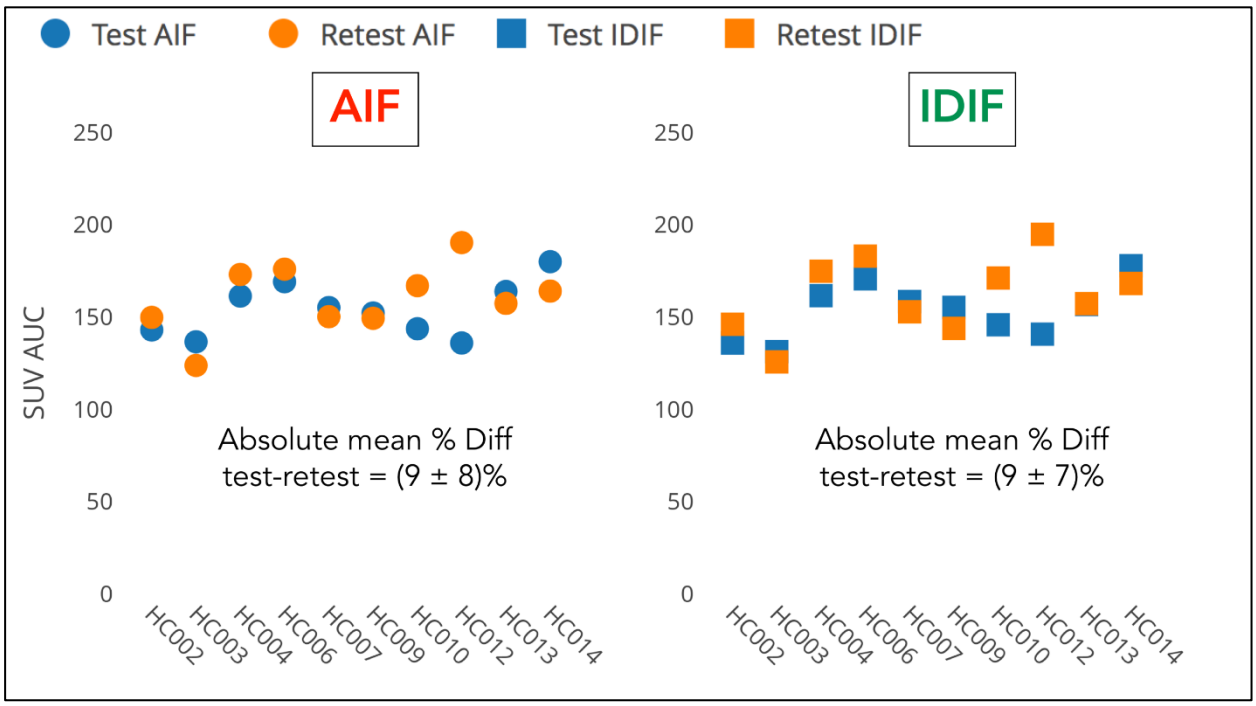

Suppl. Fig. 6. Test-retest variability of input functions normalized to body weight and injected dose (SUV). The area-under-the curve was used as a similarity metric. The intra-variability of AIF and IDIF SUV curves in terms of absolute mean % difference was similar at ((9 ± 8) %, left) and ((9 ± 7) %, right) respectively.

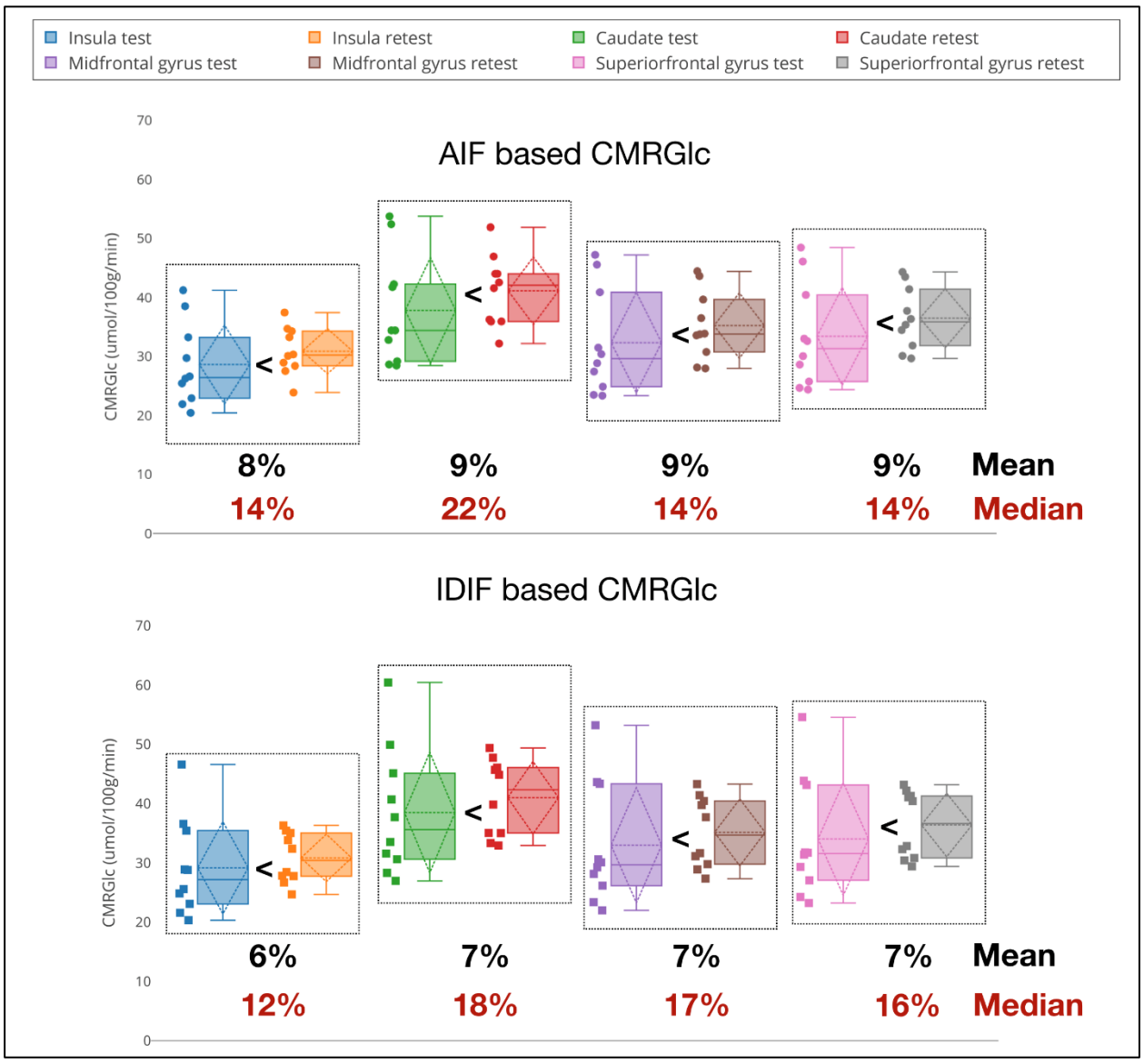

Suppl. Fig. 7. Test-retest CMRGlc variability is depicted here. Four reference regions were chosen at random (Insula, Caudate, Mid-frontal gyrus and superior frontal gyrus). AIF

based CMRGlc values for test-retest scans were plotted for these four regions (top), it can be seen that the variance (dotted lines) is lower in the retest scans, however the mean and median CMRGlc values were higher. The increase in mean (black) and median (brown) between test and retest scans are reported in terms of absolute percentage differences. This test-retest trend is seen in the IDIF based CMRGlc values as well (bottom).

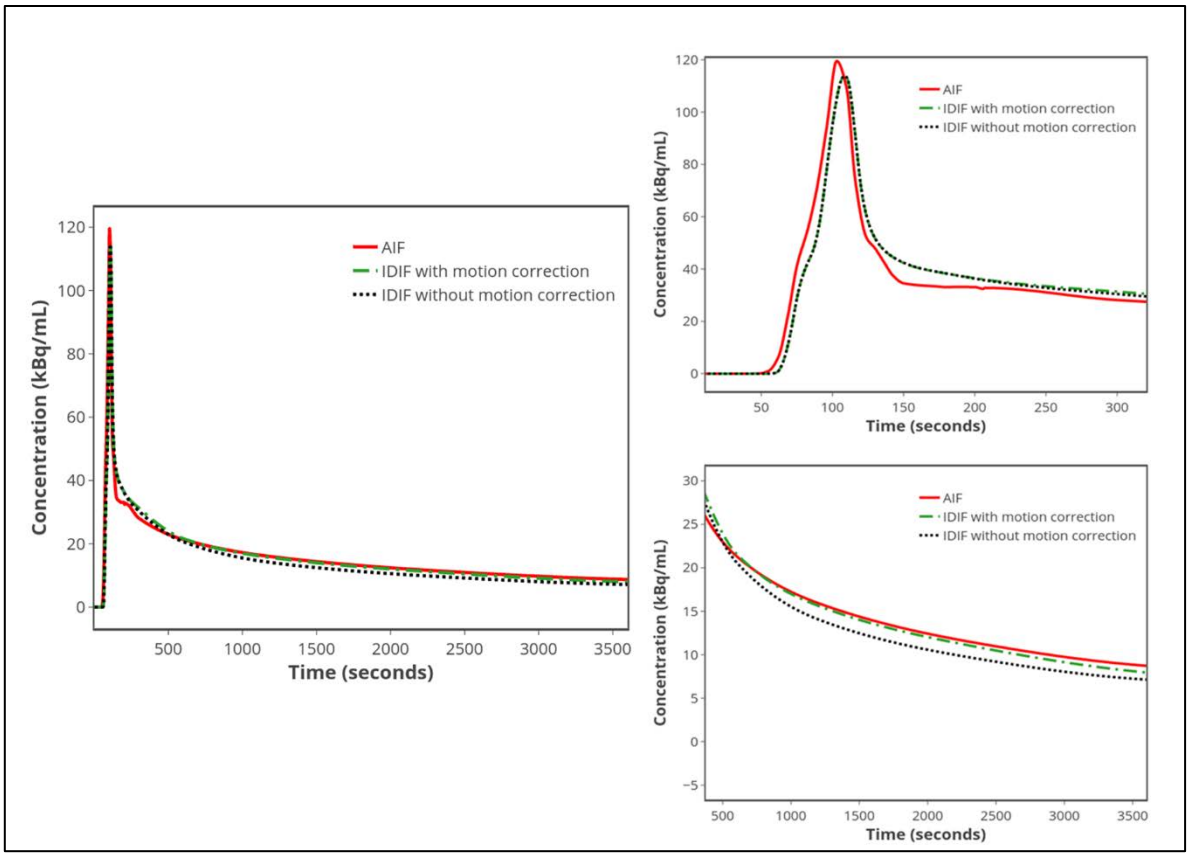

Suppl. Fig. 8. Influence of motion on IDIF (HC014 test scan, Table 1): AIF (red), IDIF with motion correction (MoCo IDIF, dashed green line) and IDIF without motion correction (no-MoCo IDIF, dotted black line). It can be seen that the MoCo IDIF has a better agreement with the AIF in comparison to the no-MoCo IDIF. The percentage difference between MoCo IDIF and the AIF was 1%, whereas the percentage difference between no-MoCo IDIF and the AIF was found to be 9%. The graph also indicates that by accounting for

involuntary subject motion, the agreement between the IDIF and AIF is significantly improved.

Supplementary Figure 9. Histogram showing the average plasma-to-blood ratio of FDG tracer concentration obtained from all the 20 subjects studied (top). Group analysis for all the 20 datasets, where the average plasma to blood ratio was found to be 1.06 ± 0.01. (bottom)

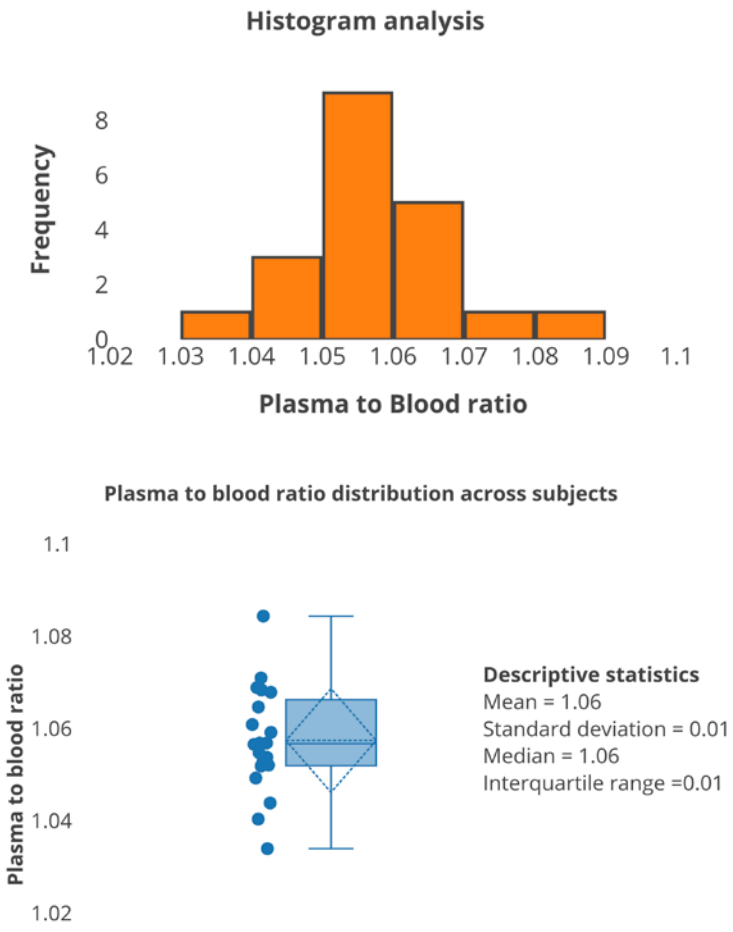

Supplementary Figure 10. (A) Whole brain CMRGlc for 20 datasets calculated using AIF (blue) and IDIF (orange), (B) Scatter plot depicting the individual whole brain CMRGlc values, where the shaded rectangle indicates same subject, with its height representing the difference between test and retest.

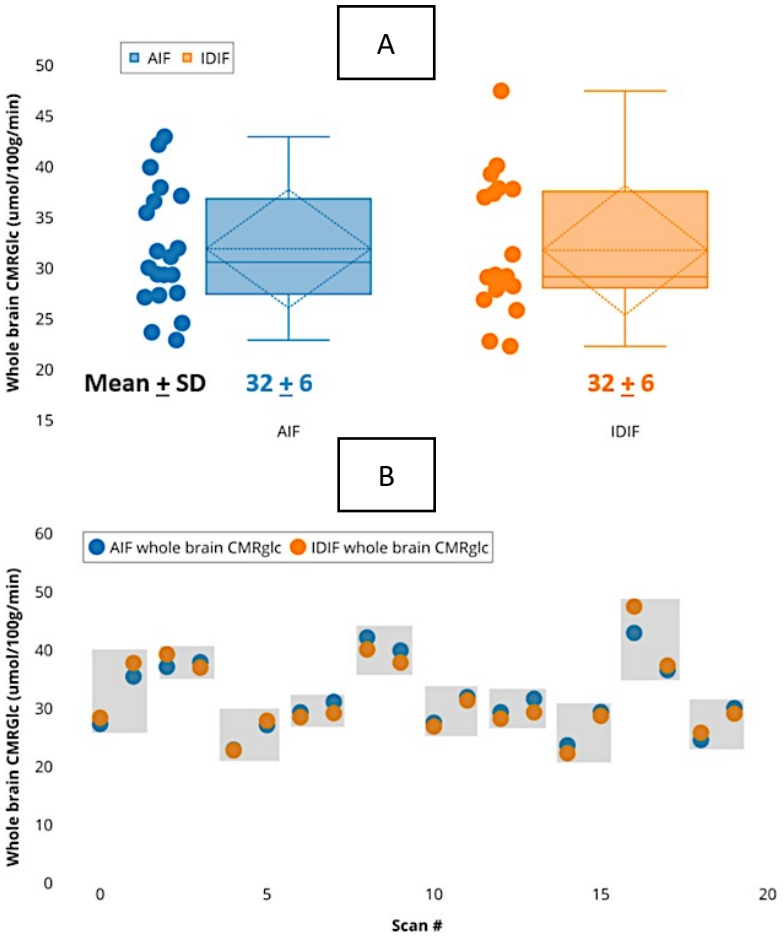

Supplementary Figure 11. Absolute relative % difference between test-retest Global CMRGlc calculated using AIF (blue) and IDIF (orange).

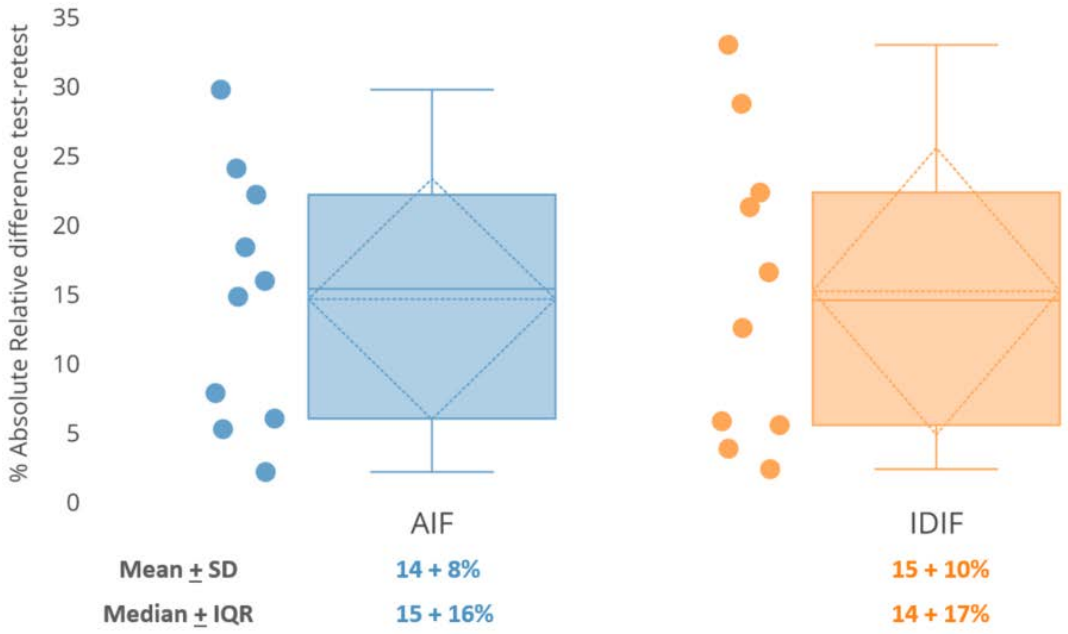

Supplementary tables

Suppl. Table. 1. Intra-frame motion (IFM) in PET frames as estimated from simultaneously acquired MR navigators was found to be negligible (<1 mm). Of note, the IFM increases

with the duration of the study.

Intra-frame translation (mm)	**10-20 min**	**20-40 min**	**40-60 min**
X direction	-0.06 $\pm$ 0.25	-0.01 $\pm$ 0.18	-0.17 $\pm$ 0.80
Y direction	0.02 $\pm$ 0.12	0.02 $\pm$ 0.12	0.12 $\pm$ 0.45
Z direction	0.03 $\pm$ 0.22	0.02 $\pm$ 0.27	0.08 $\pm$ 0.40